Check for updates

Hydrosilylation-derived silicon-containing hydrocarbon-based polymers exhibiting ultralow dielectric losses and high thermal stabilities†

Yuka Azuma, [a] Riku Takahashi, [a] Natsuko Sashi,[a] Kan Hatakeyama-Sato, [a] Yuta Nabae, [a] Ririka Sawada, [b] Shinji Ando [b] and Teruaki Hayakawa ★[a]

With the continual evolution of high-frequency communication technologies, the demand for advanced insulating materials with minimal dielectric losses has become increasingly critical. In this work, silicon-containing hydrocarbon-based polymers are prepared *via* a hydrosilylation polymerization reaction between dihydrosilanes and diynes or dienes, which are strategically engineered to achieve both a low dielectric constant (D_k) and an exceptionally low dielectric loss tangent (D_f). This polymerization method proceeded efficiently under mild conditions, yielding high-purity polymers without by-product formation. The resulting materials exhibited outstanding dielectric properties, with D_k values of ∼2.6 and D_f values <0.002 at 20 GHz, the latter of which reached as low as 0.0011 in optimized systems. Notably, these favorable characteristics were maintained even at frequencies exceeding 75 GHz. Thermogravimetric analysis confirmed excellent thermal stabilities, with decomposition temperatures (T_{d-10}) surpassing 400 °C. Moreover, the polymers displayed good solubilities in a wide range of organic solvents (excluding alcohols), indicating their practical processability. Collectively, these results demonstrate the potential of the synthesized materials for use as next-generation interlayer dielectrics for high-speed communication applications.

Introduction

The rapid proliferation of smartphones and Internet of Things (IoT) devices has significantly advanced the global information infrastructure, driving the demand for high-speed, high-capacity communication systems. To accommodate these requirements, electrical signals are increasingly operated in the high-frequency regime. However, in this regime, dielectric losses in the insulating materials used to construct the interlayer dielectrics are a critical concern. Since the dielectric loss is proportional to the square root of the dielectric constant ($D_k^{1/2}$) and the dielectric loss tangent (D_f), minimizing both parameters is essential to mitigating signal attenuation in next-generation devices.

Previously, polyimides have been widely adopted as interlayer dielectrics due to their outstanding thermal resistances and mechanical strengths.[1–3] However, their molecular polarities and ability to form charge transfer complexes often result in relatively high D_k and D_f values,[4] which typically exceed the stringent thresholds for next-generation electronics (*i.e.*, $D_k \leq 2.5$ and $D_f \leq 0.002$).[4,5] For instance, Kapton-H exhibits a D_k value of ∼3.5 and a D_f value of ∼0.01,[6,7] thereby underscoring the need for alternative materials.

Molecular design strategies for lowering D_k often involve increasing the molar volume and reducing the polarizability,[8,9] whereas reducing a D_f value requires suppression of the polymer chain mobility and the vibrational motion.[6,10] Furthermore, since water has a D_k of ∼78, moisture absorption by polymers not only elevates D_k, but may also enhance the chain dynamics *via* plasticization.[6,7,11] Therefore, designing polymers that resist water uptake is also an important requirement.

To date, various approaches have been explored to address these complex requirements, such as the introduction of fluorinated groups,[12–15] nanoporous architectures,[16–19] aliphatic linkers,[20–22] and siloxane segments[23–27] into the polyimide backbones. Among them, fluorinated structures are highly effective in lowering both D_k and D_f owing to their low polarizability characteristics and rigid nature. However, environmental regulations related to the use of perfluoroalkyl substances have restricted their application, thereby spurring the development of fluorine-free alternatives.[28]

aDepartment of Materials Science and Engineering, School of Materials and Chemical Technology, Institute of Science Tokyo, Japan.
E-mail: hayakawa@mct.isct.ac.jp
bDepartment of Chemical Science and Engineering, School of Materials and Chemical Technology, Institute of Science Tokyo, Japan

Consequently, various other classes of polymers, including poly(phenylene ether)s,[29–33] polybenzoxazoles,[34–37] fluoropolymers,[38,39] and siloxane-based polymers[40–44] have been explored as candidate materials for low-dielectric loss applications. For instance, poly(phenylene ether)s have been reported to exhibit D_k of approximately 2.5 and D_f as low as 0.002, while polybenzoxazoles derivatives typically show D_k in the range of 2.5–3.0 and D_f between 0.01 and 0.03. Among these candidates, in particular, siloxane-based polymers have been demonstrated to exhibit low polarities, high free volumes, and excellent hydrophobicities, all of which contribute to low D_k values. However, their flexible backbones often lead to high D_f values owing to their increased degrees of molecular mobility. Suppressing the chain dynamics through incorporating rigid, non-polar frameworks (*e.g.* aromatic hydrocarbon-based units) can be an effective approach to reduce D_f value. Therefore, the combination of siloxane units (for low D_k values) with hydrocarbon segments (for low D_f values) represents a compelling molecular design strategy for the development of advanced dielectric materials.

As previously reported, the hydrosilylation polymerization between dihydrosilanes and diynes or dienes offers a promising synthetic route to such hybrid structures.[45] This reaction proceeds with a high selectivity and yield under mild conditions, and produces little to no byproducts, rendering it both efficient and environmentally benign.[46] In this context, pioneering work by Seino *et al.*[45] demonstrated that silicon-containing hydrocarbon-based polymers prepared by hydrosilylation can combine a low polarity with a high rigidity, offering a favorable dielectric behavior. However, despite their potential, reports on these systems are scarce.

Thus, in the current study, a series of silicon-containing hydrocarbon-based polymers is prepared *via* the hydrosilylation polymerization of dihydrosilanes and diynes or dienes, followed by subsequent characterization. Through the systematic analysis of five types of dihydrosilanes (including two siloxane derivatives, a double-decker silsesquioxane (DDSQ), and two aromatic phenyl-substituted monomers) the solubilities, thermal stabilities, and dielectric properties of the resulting polymers are evaluated. This work also aims to evaluate the suitability of these polymers for future applications as interlayer dielectric materials in high-frequency communication technologies.

Experimental

Materials

1,1,3,3,5,5-Hexamethyltrisiloxane (HMTS), 1,1,5,5-tetramethyl-3,3-diphenyltrisiloxane (TMDP), 1,2-bis(dimethylsilyl)benzene (1,2-DMSB), 1,4-bis(dimethylsilyl)benzene (1,4-DMSB), and 1,4-bis(dimethylvinylsilyl)benzene (MVSB) were purchased from Tokyo Chemical Industry Co., Ltd (Japan) and were distilled prior to use. 1,4-Bis(phenylethynyl)benzene (BPEB) was purchased from FUJIFILM Wako Pure Chemical Corporation (Japan) and recrystallized from toluene. DDSQ was provided by JNC Corporation (Japan) and recrystallized from toluene.

Karstedt's catalyst (platinum (0) 1,3-diethenyl-1,1,3,3-tetra-methyldisiloxane complex in xylene, Pt ~2%) was purchased from Sigma-Aldrich (USA). All other reagents and solvents were obtained from Tokyo Chemical Industry Co., Ltd, FUJIFILM Wako Pure Chemical Corporation, or AGC Inc. (Japan), and were used without further purification, as explained in the ESI.†

Methods

Proton (^{1}H), carbon (^{13}C), and silicon (^{29}Si) nuclear resonance (NMR) spectroscopy were performed on a JEOL JNM-ECS400 (400 MHz) spectrometer using CDCl$_3$ as the solvent. Size-exclusion chromatography (SEC) was performed using a SHIMADZU LC-20AD system equipped with a Shodex RI 501 RI detector and a Shodex LF 804 column. The number average molecular weights (M_n) and weight average molecular weights (M_w) were determined by SEC using a polymer/tetrahydrofuran solution at a flow rate of 1.0 mL min^{-1} at 40 °C. Calibration was performed using polystyrene standards. The thermal behaviors of the polymers were characterized using a Seiko DSC 7020 differential scanning calorimeter (DSC) at heating and cooling rates of 10 °C min^{-1} under a nitrogen flow. The glass transition temperatures (T_g) were determined from the second heating and cooling scans. The scanning temperature range was set from −30 to 250 °C. Thermogravimetric analyses (TGA, SII TGA 7300 system) were performed in the range of 30–550 °C (10 °C min^{-1} heating rate) under a flow of nitrogen. A split-cylinder resonator (20 and 40 GHz; EM Labs) equipped with a network analyzer was used to measure the D_k and D_f values. The average D_k and D_f values obtained from three measurements are provided in the text. A Fabry–Pérot resonator (75–110 GHz) (EM Labs) with a network analyzer was used to measure the D_k and D_f values. The dielectric properties of the samples were measured at ~28 °C and under 34% relative humidity (RH). A Bruker Discover D8 equipped with a Cu (1.54 Å) X-ray source was used to obtain the wide-angle X-ray diffraction (WAXD) profiles.

Synthesis of the silicon-containing hydrocarbon-based polymers

The silicon-containing hydrocarbon-based polymers were synthesized *via* hydrosilylation polymerization using dihydrosilanes, dienes, and diynes as monomers. BPEB and MVSB were employed as the diyne and diene monomers, respectively. The dihydrosilane monomers used in this study included HMTS and TMDP (featuring a siloxane backbone), DDSQ (characterized by a silsesquioxane cage structure), and 1,2-DMSB and 1,4-DMSB (polymers that allow benzene ring incorporation into the main chain). The structures of these monomers are shown in Scheme 1. For preparation of the BPEB-based system using TMDP as the hydrosilane monomer, TMDP (0.337 g, 1.0 mmol) and BPEB (0.282 g, 1.0 mmol) were placed in a test tube and purged with argon gas to create an inert atmosphere. Toluene (2 mL) was then added, and the mixture was stirred at 100 °C until achieving complete dissolution. Subsequently, a catalytic amount of Karstedt's catalyst (five drops) was added, and the mixture was stirred at 100 °C for 24 h. After this time, the polymerized reaction mixture was precipitated using a
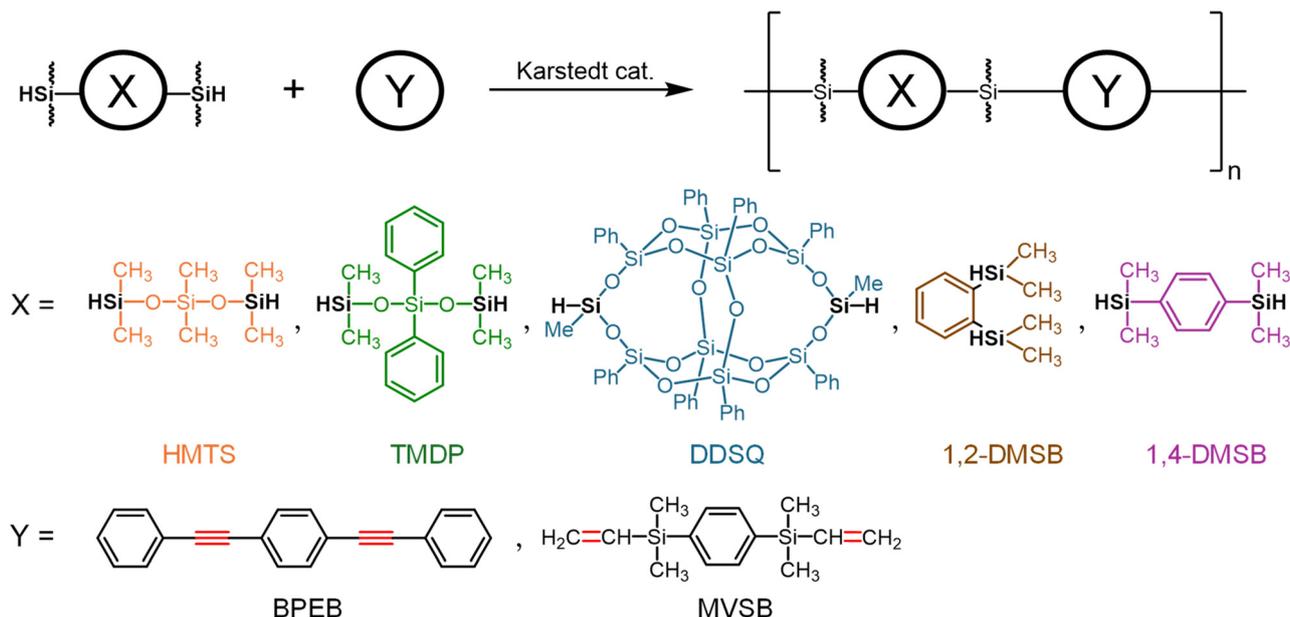
Scheme 1 Synthesis of the silicon-containing hydrocarbon-based polymers.

large excess of methanol. The resulting precipitate was collected by vacuum filtration and dried under reduced pressure at 40 °C to afford the desired polymer (0.615 g, 99%). The synthetic procedures for preparation of the other BPEB-containing polymers are described in the ESI.†

The MVSB-based system incorporating TMDP as the hydrosilane monomer was prepared using an analogous procedure. More specifically, TMDP (0.337 g, 1.0 mmol) and MVSB (0.251 g, 1.0 mmol) were placed in a test tube and purged with argon gas to create an inert atmosphere. Toluene (2 mL) was then added, and the mixture was stirred at 60 °C until achieving complete dissolution. Subsequently, a catalytic amount of Karstedt's catalyst (five drops) was added, and the mixture was stirred at 60 °C for 24 h. After this time, the polymerized reaction mixture was precipitated using a large excess of methanol. The resulting precipitate was collected by vacuum filtration and dried under reduced pressure at 40 °C to afford the desired polymer (0.512 g, 87%). The synthetic procedures for the preparation of the other MVSB-containing polymers are described in the ESI.†

Fabrication of the polymer film

For measurement of the D_k and D_f values, polymer films were prepared. More specifically, the polymers obtained in the previous steps were redissolved in toluene, and the solution concentration was adjusted to 30–35 wt%. The resulting solutions were cast onto glass substrates and spread using a film applicator. Following initial air drying of the films at room temperature (around 25 °C) for 1 h, they were subjected to vacuum drying overnight at 80 °C to ensure complete solvent removal. Subsequently, the dried films were detached from the glass substrates by immersion in warm water to obtain freestanding polymer films. The film thickness was determined using an average of 15 measurement points.

Results and discussion

Synthesis and characterization

A systematic series of silicon-containing hydrocarbon-based polymers was synthesized *via* hydrosilylation polymerization using various dihydrosilanes and either diene or diyne monomers. The resulting polymers are denoted based on the monomer pairings, such as HMTS–BPEB, wherein HMTS and BPEB represent the dihydrosilane and diyne components, respectively. The dihydrosilane monomers included flexible siloxane-based units (HMTS and TMDP), a rigid cage-like DDSQ, aromatic phenylene-bridged systems (1,2-DMSB and 1,4-DMSB), and a binary mixture of TMDP and DDSQ (molar ratio = 8 : 2) to modulate the structural rigidity and symmetry of the polymer system.

The hydrosilylation polymerization reaction was performed under equimolar conditions in toluene at elevated temperatures (typically 60–100 °C) for 24 h in the presence of Karstedt's catalyst. This platinum(0)-based catalyst is known to promote selective *cis*-addition across multiple carbon–carbon bonds, thereby enabling the efficient formation of a linear polymer with minimal side reactions.[47]

The polymerization reactions involving the diyne monomer BPEB were conducted at 100 °C to ensure complete dissolution of all components and to promote homogeneous reaction conditions. For HMTS–BPEB system, the initial use of equimolar amounts of HMTS (1.0 mmol) and BPEB (1.0 mmol) afforded a polymer with a relatively low molecular weight. This outcome was attributed to the volatility of HMTS (boiling point

= 128 °C), which may have caused its partial evaporation during the reaction performed at 100 °C, thereby disrupting the stoichiometric balance. To address this issue, the polymerization conditions were optimized by employing a slight excess of HMTS (1.1 mmol), which successfully yielded a polymer with a significantly higher molecular weight. When DDSQ was employed, polymerization at 100 °C led to gelation of the reaction solution. This observation indicates that the vinyl groups

in the polymer backbone underwent additional hydrosilylation reactions with the residual Si–H groups, leading to cross-linking. It should be noted that such crosslinking side reactions may also occur with other monomers, although gelation was not observed in those systems. Therefore, for DDSQ-based systems, the reactions were conducted at 60 °C.

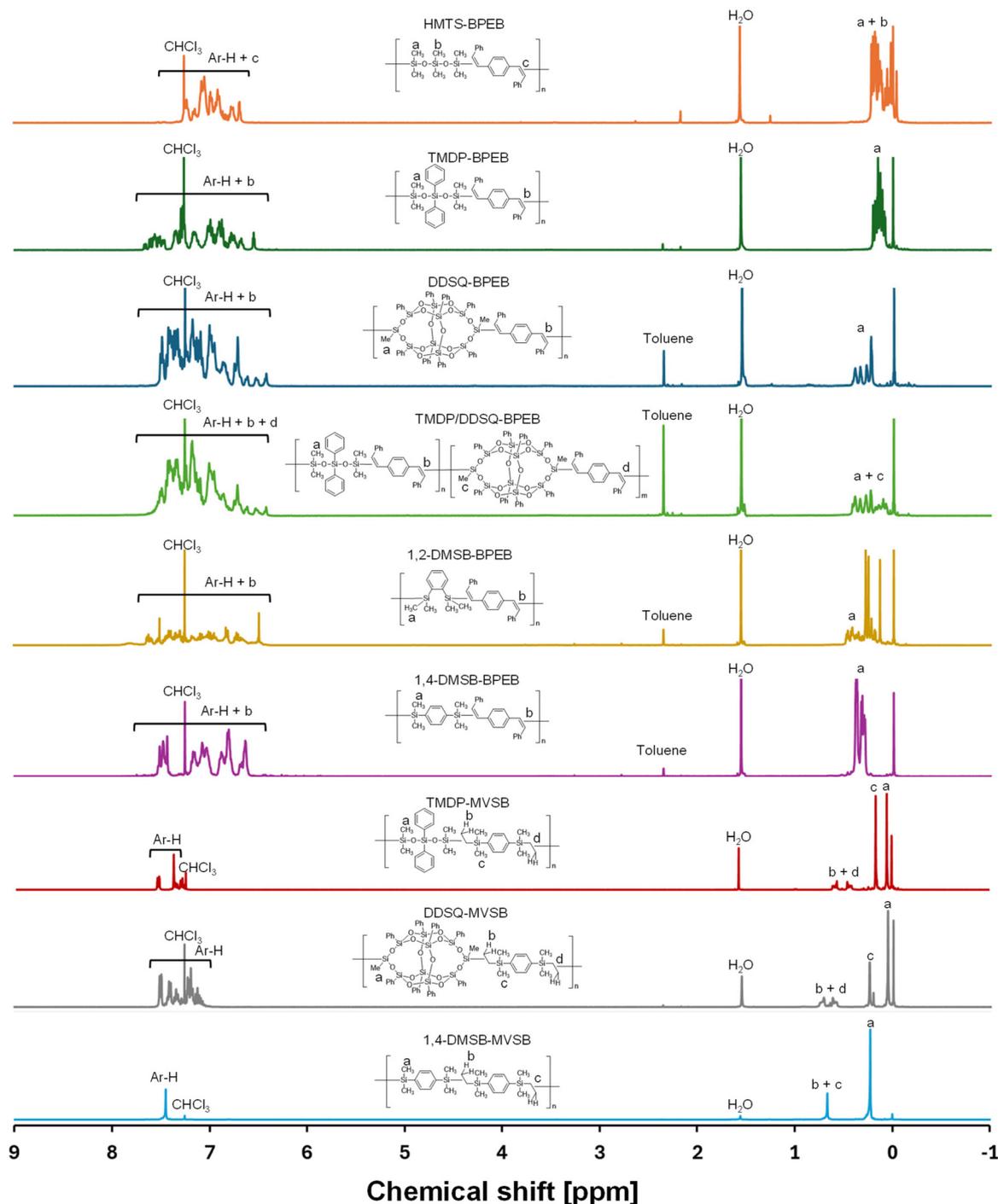The structures of the prepared polymers were confirmed using ^{1}H NMR spectroscopy, as shown in Fig. 1. For all

Fig. 1 ^{1}H NMR spectra of the silicon-containing hydrocarbon-based polymers.

polymer samples, the disappearance of the Si–H signals between 4.0 and 5.0 ppm and the complete assignment of the remaining peaks indicated near-quantitative conversion. A more detailed ^{1}H NMR spectrum of TMDP–BPEB is shown in Fig. S1,† wherein it can be seen that the Si–H peak originally observed at ~4.8 ppm in the TMDP spectrum completely disappeared after polymerization. In addition, the signals observed at 0.05–0.2 ppm were attributed to the methyl groups bonded to the silicon atoms in the TMDP unit. Furthermore, the signals detected between 6.5–7.6 ppm were assigned to the vinyl protons and the aromatic protons. To further confirm the chemical structure, ^{13}C NMR and ^{29}Si NMR analyses were also conducted, as shown in Fig. S2 and S3,† respectively.

The molecular weights determined by SEC are summarized in Table 1, while the corresponding SEC traces are shown in Fig. S4.† All polymers except those derived from 1,2-DMSB exhibited moderate-to-high molecular weights, with M_n values ranging from 14.7 to 70.5 kg mol^{-1} and M_w values ranging from 28.8 to 252 kg mol^{-1}. Notably, the 1,2-DMSB–BPEB polymer exhibited a relatively low molecular weight (M_n = 1.44 kg mol^{-1}), likely due to intramolecular steric hindrance between the two closely spaced Si–H groups, which suppressed chain propagation. Accordingly, 1,2-DMSB–BPEB cannot be regarded as a high-molecular-weight polymer and was therefore excluded from physical property measurements.

Subsequent polymerization with the diene monomer MVSB was conducted using TMDP, DDSQ, and 1,4-DMSB, each of which was previously identified to yield high-molecular-weight polymers with BPEB. These polymerization reactions were carried out at 60 °C to minimize side reactions. As for the BPEB-based polymers, ^{1}H NMR analysis confirmed complete consumption of the Si–H groups, and SEC revealed M_n values ranging from 21.3 to 75.0 kg mol^{-1} along with M_w values ranging from 44.2 to 170 kg mol^{-1}, consistent with successful linear polymer formation.

Thermal properties of the silicon-containing hydrocarbon-based polymers

The thermal stabilities and glass transition behaviors of the polymers were subsequently evaluated using TGA and DSC. The 10% weight loss temperature (T_{d-10}) and the glass transition temperature (T_g) are summarized in Table 1, and the representative TGA and DSC curves are shown in Fig. 2 and 3, respectively. All polymers displayed excellent thermal stabilities, with T_{d-10} values exceeding 400 °C. DDSQ–MVSB exhibited the highest T_{d-10} value (538 °C), reflecting the thermal resilience of its rigid silsesquioxane cage. Although 1,4-DMSB–BPEB demonstrated the lowest T_{d-10} within the series (*i.e.*, 407 °C), this value continued to reflect a high thermal stability. It was also found that the T_g values varied significantly depending on the rigidity of the polymer backbones. More specifically, DDSQ-containing polymers exhibited notably
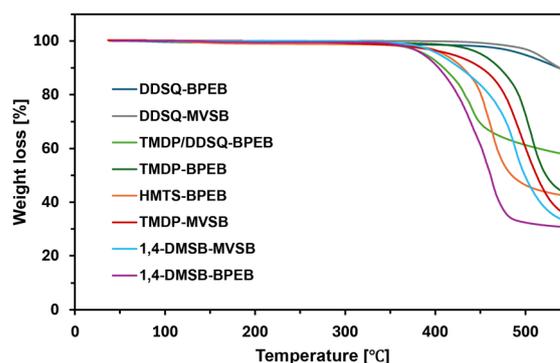
Fig. 2 TGA curves of the silicon-containing hydrocarbon-based polymers.

Fig. 3 DSC curves of the silicon-containing hydrocarbon-based polymers.

Table 1 Characteristics of the silicon-containing hydrocarbon-based polymers

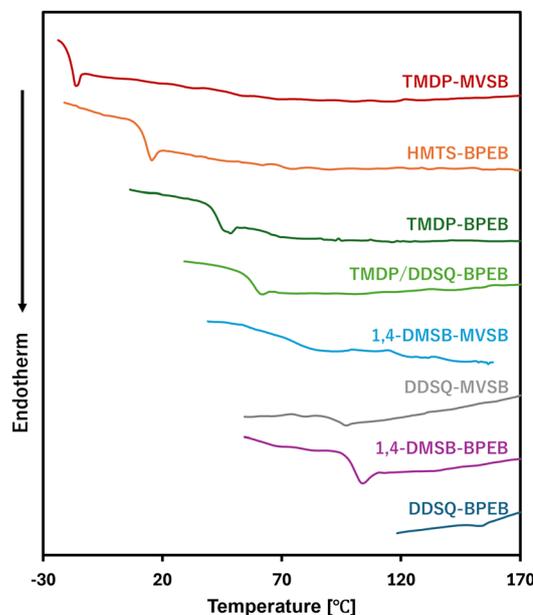| Sample	$M_n{}^a$ (kg mol^{-1})	$M_w{}^a$ (kg mol^{-1})	$T_{d-10}{}^b$ (°C)	$T_g{}^c$ (°C)
HMTS–BPEB	14.7	28.8	431	13
TMDP–BPEB	70.5	252	471	41
DDSQ–BPEB	42.8	81.7	537	161
TMDP/DDSQ–BPEB^d	72.2	165	409	55
1,2-DMSB–BPEB	1.44	1.60	—	—
1,4-DMSB–BPEB	33.4	63.7	407	100
TMDP–MVSB	40.6	170	451	−18
DDSQ–MVSB	75.0	148	538	91
1,4-DMSB–MVSB	21.3	44.2	427	84

^{a} Determined by SEC measurements in tetrahydrofuran (THF), using a Shodex LF 804 column at 40 °C. Calibration was performed using polystyrene standards. ^{b} Determined by TGA in N$_2$ at a heating rate of 10 °C min^{-1}. ^{c} Determined by DSC in N$_2$ at a heating rate of 5 °C min^{-1}. ^{d} Polymer obtained by reacting TMDP and DDSQ (8 : 2 molar ratio) with BPEB.

higher T_g values (160 °C for DDSQ–BPEB and 91 °C for DDSQ–MVSB), consistent with their restricted chain mobilities caused by the cage-like DDSQ structure. Conversely, the siloxane-based polymers exhibited relatively low T_g values (13 °C for HMTS–BPEB and −18 °C for TMDP–MVSB), which were attributed to their flexible siloxane backbones. This trend aligns with literature values, including the T_g of polydimethylsiloxane, which was reported to be −123 °C.[48]

A clear distinction was observed between the polymers derived from the diyne (BPEB) and diene (MVSB) monomers, wherein the polymers derived from MVSB exhibited consistently lower T_g values than their BPEB counterparts. BPEB initially possesses rigid triple bonds and a fully conjugated aromatic system. Upon hydrosilylation, the triple bonds are converted to double bonds while maintaining molecular rigidity, which restricts molecular motion and leads to higher T_g values. In contrast, MVSB forms single bonds upon hydrosilylation, resulting in greater chain flexibility and lower T_g values. These results suggest that precise control over the rigidity and connectivity of monomer units is crucial for tuning the thermal properties of silicon-containing hydrocarbon-based polymers.

Additionally, in the DSC curve of 1,4-DMSB–MVSB, endothermic peaks were observed at 176 and 189 °C during the heating process, while an exothermic peak appeared at 158 °C during the cooling process (Fig. S5†). These thermal events are believed to correspond to phase transitions arising from the ordered aromatic segments within the polymer.

Solubilities of the silicon-containing hydrocarbon-based polymers

Qualitative solubility tests were conducted to evaluate the fundamental chemical properties of the synthesized polymers. As summarized in Table 2, the majority of polymers were insoluble in protic polar solvents such as ethanol, but showed good solubilities in aprotic polar solvents such as tetrahydrofuran (THF) and N,N-dimethylformamide (DMF). Additionally, the polymers exhibited good solubilities in non-polar solvents such as toluene, and halogenated solvents such as dichloromethane (DCM). These solubility characteristics were found to

be strongly dependent on the molecular structures of the polymers, and the low polarity characteristics of the prepared polymers were believed to contribute to their hydrophobic nature. Notably, the polymers derived from siloxane-based monomers (e.g., HMTS and TMDP) exhibited slightly enhanced solubilities compared to the other polymers. This behavior can be attributed to the flexible nature of the siloxane segments, which increase the chain flexibility and reduce the extent of intermolecular interactions, thereby improving the solubility. In contrast, 1,4-DMSB–MVSB was insoluble in most solvents at room temperature (around 25 °C) and was only slightly soluble in THF and DCM upon heating. This is likely due to its higher degree of crystallinity, as estimated from the DSC measurements (Fig. S5†).

WAXD analysis of the silicon-containing hydrocarbon-based polymers

The higher-order structures of the synthesized polymers were analyzed using WAXD, and the results are shown in Fig. 4. It can be seen that HMTS–BPEB, TMDP–BPEB, 1,4-DMSB–BPEB, and TMDP–MVSB exhibited no distinct diffraction peaks, indicating amorphous morphologies without long-range order. In contrast, polymers containing DDSQ (e.g., DDSQ–BPEB) exhibited a clear diffraction peak in the 2θ region of 7.8–8.0°, corresponding to a d-spacing of ~1.0–1.1 nm. In addition, a broad amorphous halo was observed in the wide-angle region. This feature is consistent with the molecular dimensions of the DDSQ cage structure, suggesting that its periodicity was retained within the polymer backbone after polymerization. These observations support the notion that the DDSQ unit forms locally ordered domains even in the absence of an overall crystallinity.

Additionally, 1,4-DMSB–MVSB displayed distinct diffraction peaks at 2θ values of ~15 and 20°, corresponding to d-spacings of approximately 0.60 and 0.44 nm, respectively. The d-spacing of 0.60 nm likely reflects the repeating unit along the polymer chain, as illustrated in Fig. S6.† In contrast, the d-spacing of 0.44 nm may be attributed to the interchain distance between polymer backbones. Collectively, these results indicate that while most of the synthesized polymers are amorphous, local

Table 2 Solubility of the silicon-containing hydrocarbon-based polymers

Solubility[a]

Sample	EtOH[b]	THF	DMF	DMSO[b]	Toluene	Acetone	Hexane	EtOAc[b]	DCM
HMTS–BPEB	−	+	+	−	+	+	+	+	+
TMDP–BPEB	−	+	+	−	+	±	±	+	+
DDSQ–BPEB	−	+	+	−	+	±	-	+	+
TMDP/DDSQ–BPEB[c]	−	+	+	−	+	±	±	+	+
1,4-DMSB–BPEB	−	+	+	−	+	±	±	+	+
TMDP–MVSB	−	+	+	−	+	+	+	+	+
DDSQ–MVSB	−	+	+	−	+	+	−	+	+
1,4-DMSB–MVSB	−	+h	−	−	−	−	−	−	+h

[a] +: Soluble at room temperature; +h: soluble upon heating; ±: partially soluble; −: insoluble even upon heating. [b] EtOH, ethanol; DMSO, dimethyl sulfoxide; EtOAc, ethyl acetate. [c] Polymer obtained by reacting TMDP and DDSQ (8 : 2 molar ratio) with BPEB.
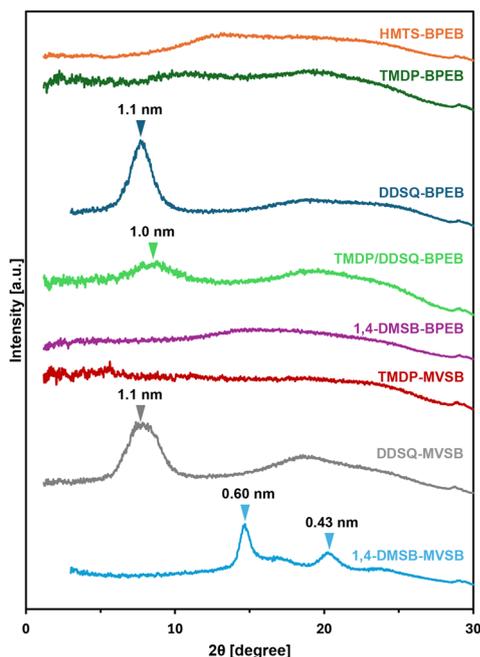
Fig. 4 WAXD profiles of the silicon-containing hydrocarbon-based polymers.

Fig. 5 Photographic images of the self-supporting polymer films: (a) TMDP–BPEB, (b) TMDP/DDSQ–BPEB, (c) 1,4-DMSB–BPEB, and (d) DDSQ–MVSB.

structural features, especially those introduced by DDSQ or rigid aromatic segments, can generate periodicity that is observable by WAXD.

Fabrication of the polymer films

For measurement of the polymer D_k and D_f values, self-supporting polymer films were prepared by solution casting. Notably, the TMDP–BPEB, TMDP/DDSQ–BPEB, 1,4-DMSB–BPEB, and DDSQ–MVSB polymers yielded uniform, freestanding films upon solvent evaporation and water assisted detachment from the glass substrates, as shown in Fig. 5.

In contrast, HMTS–BPEB and TMDP–MVSB remained tacky at room temperature because of their low T_g values, thereby rendering them unsuitable for freestanding film formation. Additionally, DDSQ–BPEB exhibited partial cracking, likely caused by the high rigidity of both the DDSQ and BPEB units, which reduced the film flexibility and the stress relaxation behavior during drying. Notably, 1,4-DMSB–MVSB could not be processed into a film because of its limited solubility, which prevented uniform casting. These results highlight that the film formability is governed not only by the thermal and solubility properties of the polymers, but also by the interplay between the backbone rigidity and the chain flexibility. An optimal balance between these factors is therefore essential for the production of defect-free processable dielectric films.

Dielectric properties of the silicon-containing hydrocarbon-based polymers

The dielectric properties of the synthesized polymers were evaluated to assess their potential use for low dielectric loss
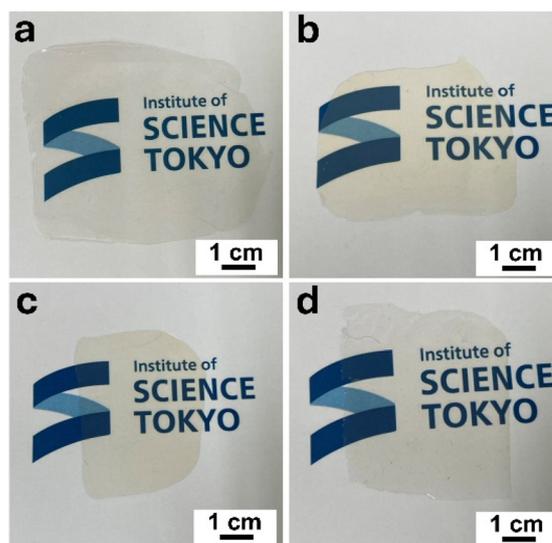
materials. For this purpose, four films, namely those based on the TMDP–BPEB, TMDP/DDSQ–BPEB, 1,4-DMSB–BPEB, and DDSQ–MVSB polymers, were successfully fabricated and subjected to dielectric measurements. The D_k and D_f values were measured at 20 and 40 GHz, and the results are summarized in Table 3. Additionally, representative 20 GHz values are shown in Fig. 6(a) and (b), wherein each presented value represents an average of three measurements. It was found that all polymers exhibited D_k values of approximately 2.6 at both 20 and 40 GHz, which are significantly lower than that of the conventional polyimide Kapton-H ($D_k \approx 3.5$).[6,7] Furthermore, the obtained D_k values are comparable to those of both polyphenylene ether (PPE, $D_k \approx 2.5$),[29–32] and polybenzoxazole (PBO) derivatives ($D_k \approx 2.5$–3.0).[34–37] These relatively low D_k values were attributed to the incorporation of DDSQ and silicon-based components such as siloxane (TMDP), which are known to increase the free volume and thereby lower the dielectric constant. In addition, the absence of highly ordered structures, as suggested by WAXD analysis, is presumed to con-

Table 3 Dielectric properties of the silicon-containing hydrocarbon-based polymers

Sample	$D_k{}^a$		$D_f{}^a$	
	20 GHz	40 GHz	20 GHz	40 GHz
TMDP–BPEB	2.62	2.64	0.0011	0.0014
TMDP/DDSQ–BPEB^b	2.67	2.67	0.0011	0.0015
1,4-DMSB–BPEB	2.66	2.69	0.0012	0.0013
DDSQ–MVSB	2.65	2.69	0.0020	0.0021

^{a} D_k and D_f were measured using a split cylinder resonator at 20 GHz and 40 GHz, respectively. ^{b} Polymer obtained by reacting TMDP and DDSQ (8:2 molar ratio) with BPEB.
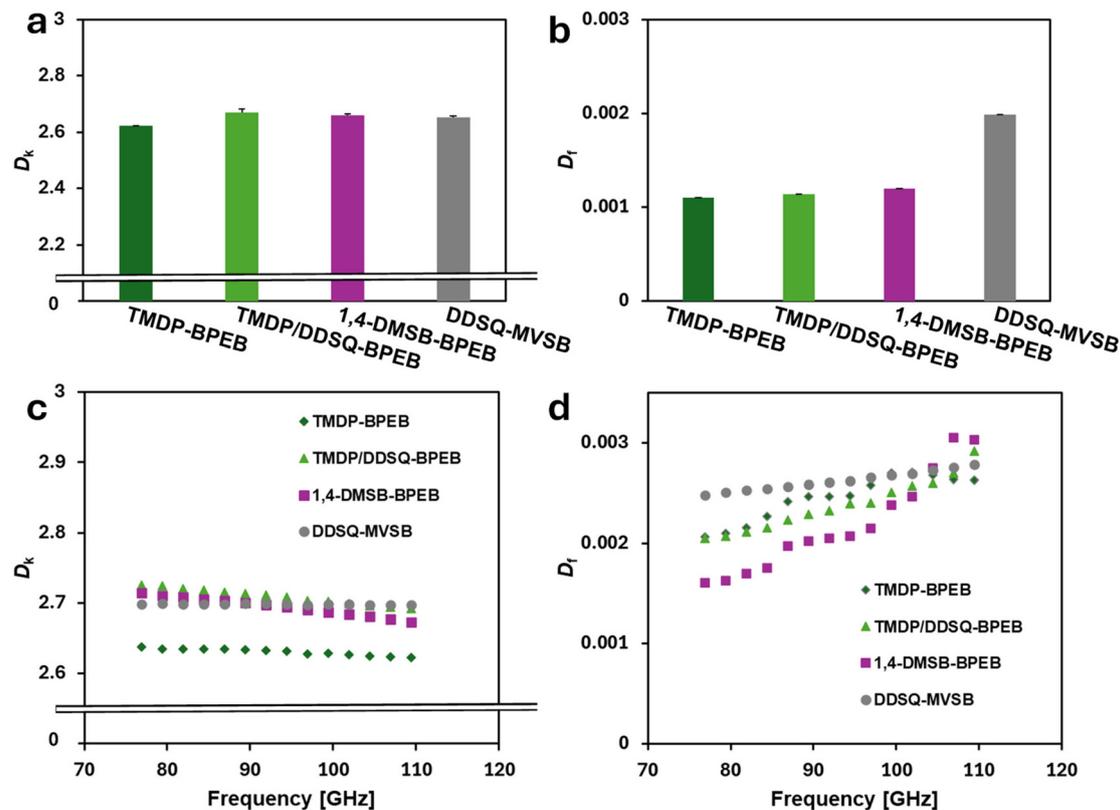
Fig. 6 (a) Dielectric constants of the polymers at 20 GHz, (b) dielectric loss tangents of the polymers at 20 GHz, (c) dielectric constants and (d) dielectric loss tangents of the polymers recorded at different frequencies.

tribute to the increase in free volume, further reducing the D_k. Indeed, previous studies have reported that the inclusion of siloxane or DDSQ units in polyimide structures results in a reduction in D_k.[23-27,49]

Even more notable were the exceptionally low D_f values, all of which were <0.002. More specifically, the TMDP–BPEB and TMDP/DDSQ–BPEB samples exhibited the lowest D_f values, reaching 0.0011 at 20 GHz. Notably, this value is approximately one-tenth that of Kapton-H ($D_f = 0.01$),[6,7] and lower than those of both PPE ($D_f \approx 0.002$)[29-33] and PBO derivatives ($D_f \approx 0.01$–0.02).[34-37] This result is likely to be due to the use of monomers lacking polar functional groups such as amide, ester, and imide units, along with the use of symmetric molecular structures, which helps to suppress anisotropic molecular vibrations and thereby reduce D_f. Moreover, these polymers are hydrocarbon-based materials that exhibit an inherent hydrophobicity and, therefore, possess a limited water uptake capability.[50,51] Consequently, the observed low polarity and reduced water uptake capability were also considered to contribute to the excellent dielectric performances of these materials. In contrast, DDSQ–MVSB demonstrated a slightly higher D_f value than the BPEB-based polymers. This behavior is attributable to the increased flexibility of the polymer chains following conversion of the MVSB double bonds to single bonds during the hydrosilylation reaction, which may enhance the degree of segmental motion.

Fluorinated polymers such as PTFE (polytetrafluoroethylene) exhibit even lower dielectric properties, with a D_k of approximately 2.1 and a D_f of about 0.0003.[52] However, their application has been increasingly constrained due to growing environmental concerns, particularly regarding the regulation of perfluoroalkyl substances. In this context, the silicon-containing hydrocarbon-based polymers developed in this study represent promising perfluoroalkyl-free alternatives, achieving sufficiently low dielectric loss.

Due to the fact that the dielectric loss ($D_k^{1/2} \cdot D_f$) is proportional to the square root of D_k and the value of D_f, the synthesized polymers exhibited extremely low overall dielectric loss values of <0.01. Notably, TMDP–BPEB demonstrated the lowest $D_k^{1/2} \cdot D_f$ value of 0.0018 at 20 GHz, while the highest (but still extremely low) value was observed for DDSQ–MVSB (i.e., 0.0032), indicating the excellent dielectric performances of these materials.

To further investigate the applicability of these materials in future wireless communication technologies, wherein frequencies >100 GHz are expected, dielectric measurements were conducted in the frequency range of 75–110 GHz. As presented in Fig. 6(c) and (d), even at these high frequencies, all polymers maintained low D_k and D_f values, which are comparable to those observed at 20 and 40 GHz. Although D_k showed a negligible frequency dependence, D_f exhibited a slight increase with increasing frequency. This trend is consistent with pre-

vious reports on polyimides, and can be attributed to the molecular vibrational modes of the polymeric structures.[53]

Interestingly, no direct correlation was observed between T_g and D_f. For instance, TMDP–BPEB, which exhibited a relatively low T_g of 41 °C, achieved the lowest D_f value of 0.0011 at 20 GHz, while DDSQ–MVSB, despite its higher T_g of 91 °C, showed a slightly higher D_f of 0.0020 at 20 GHz. These results suggest that factors such as hydrophobicity, molecular symmetry, and suppression of dipolar relaxation play dominant roles in determining the D_f values of the prepared materials. It is also possible that other factors, particularly the polymer resistance to moisture absorption, may play a significant role, since water molecules are known to affect D_f. As described above, solubility tests confirmed that the synthesized polymers were insoluble in protic solvents such as ethanol, indicating a low affinity for moisture. This hydrophobic character likely contributes to the suppression of water uptake, helping maintain a low D_f value. Furthermore, the use of symmetric monomer structures may also help suppress D_f by reducing local dipolar fluctuations. Thus, in addition to controlling the chain mobility, minimizing moisture absorption and employing structurally symmetric units appear to be important factors for achieving ultralow D_f values.

Overall, the silicon-containing hydrocarbon-based polymers synthesized in this study demonstrated excellent dielectric properties even in the high-frequency range. These results suggest that these materials are promising candidates for use as low-dielectric-loss materials in next-generation high-speed communication technologies.

Conclusions

In this study, a series of silicon-containing hydrocarbon-based polymers were successfully synthesized *via* a hydrosilylation polymerization protocol between dihydrosilanes and diynes or dienes to generate novel low-dielectric-loss materials. The resulting polymers exhibited excellent dielectric performances, including low dielectric constants ($D_k \approx 2.6$) and ultralow dielectric loss tangents ($D_f < 0.003$) at high frequencies of up to 110 GHz. Notably, the TMDP–BPEB (1,1,5,5-tetramethyl-3,3-diphenyltrisiloxane combined with 1,4-bis(phenylethynyl) benzene) and the TMDP/DDSQ–BPEB (TMDP combined with a double-decker silsesquioxane and BPEB) polymers achieved exceptionally low D_f values of 0.0011 at 20 GHz, representing significantly lower values than the target D_f that is typically required for interlayer dielectric materials. Although no direct correlation was found between the glass transition temperature and D_f, other factors, such as molecular hydrophobicity, backbone symmetry, and suppression of dipolar relaxation, were found to play dominant roles in minimizing the D_f. The inherent resistances of these polymers to moisture absorption, as confirmed by their insoluble nature in protic solvents, likely contributed to the suppression of water-induced D_f. Moreover, the use of structurally symmetric monomers appeared to reduce local dipolar fluctuations, further enhancing the dielec-

tric performance. Collectively, these findings highlight the effectiveness of combining low-polarity siloxane and rigid hydrocarbon segments in the design of novel polymers. The materials reported herein show significant potential for use as low-loss interlayer dielectric materials in emerging high-frequency communication technologies.

Author contributions

Conflicts of interest

The authors declare no other conflicts of interest.

Data availability

The data supporting this article have been included as part of the article and its ESI.†

Acknowledgements

References

1 A. Georgiev, D. Dimov, E. Spassova, J. Assa, P. Dineff and G. Danev, in *High Performance Polymers – Polyimides Based - From Chemistry to Applications*, IntechOpen, 2012.

2 D.-J. Liaw, K.-L. Wang, Y.-C. Huang, K.-R. Lee, J.-Y. Lai and C.-S. Ha, *Prog. Polym. Sci.*, 2012, **37**, 907–974.

3 A. Pașahan, in *High Perform. Polym*, IntechOpen, 2012.

4 G. Maier, *Prog. Polym. Sci.*, 2001, **26**, 3–65.

5 W. Volksen, R. D. Miller and G. Dubois, *Chem. Rev.*, 2010, **110**, 56–110.

6 C.-C. Kuo, Y.-C. Lin, Y.-C. Chen, P.-H. Wu, S. Ando, M. Ueda and W.-C. Chen, *ACS Appl. Polym. Mater.*, 2021, **3**, 362–371.

7 R. Sawada and S. Ando, *J. Phys. Chem. C*, 2024, **128**, 6979–6990.

8 Z. Ahmad, in *Dielectric Material*, IntechOpen, 2012.

9 D. W. Van Krevelen and K. Te Nijenhuis, *Properties of Polymers*, Elsevier, 2009, pp. 525–597.

10 H. Araki, Y. Kiuchi, A. Shimada, H. Ogasawara, M. Jukei and M. Tomikawa, *J. Photopolym. Sci. Technol.*, 2020, **33**, 165–170.

11 R. Bei, K. Chen, Q. Liu, Y. He, C. Li, H. Huang, Q. Guo, Z. Chi, J. Xu, Z. Chen, S. Liu and Y. Zhang, *Macromolecules*, 2024, **57**, 2142–2153.

12 L. Luo, T. Qiu, Y. Meng, L. Guo, J. Yang, Z. Li, X. Cao and X. Li, *RSC Adv.*, 2013, **3**, 14509–14520.

13 S.-J. Park, K.-S. Cho and S.-H. Kim, *J. Colloid Interface Sci.*, 2004, **272**, 384–390.

14 L. Tao, H. Yang, J. Liu, L. Fan and S. Yang, *Polymer*, 2009, **50**, 6009–6018.

15 Z. Wang, M. Zhang, E. Han, H. Niu and D. Wu, *Polymer*, 2020, **206**, 122884.

16 J. L. Hedrick, T. P. Russell, J. Labadie, M. Lucas and S. Swanson, *Polymer*, 1995, **36**, 2685–2697.

17 F. Lv, L. Liu, Y. Zhang and P. Li, *J. Appl. Polym. Sci.*, 2015, **132**, 41480.

18 S. Mehdipour-Ataei and E. Aram, *Adv. Polym. Technol.*, 2014, **33**, 21407–21418.

19 W.-C. Wang, R. H. Vora, E.-T. Kang, K.-G. Neoh, C.-K. Ong and L.-F. Chen, *Adv. Mater.*, 2004, **16**, 54–57.

20 Y. Watanabe, Y. Sakai, Y. Shibasaki, S. Ando, M. Ueda, Y. Oishi and K. Mori, *Macromolecules*, 2002, **35**, 2277–2281.

21 S. Yu, J. Zhou, A. Xu, J. Lao, H. Luo and S. Chen, *Chem. Eng. J.*, 2023, **469**, 143803.

22 M.-C. Mi, F.-E. Szu, Y.-C. Cheng, C.-H. Tsai, J.-H. Chen, J.-H. Huang, C.-C. Kuo, Y.-C. Lin, M. Leung and W.-C. Chen, *ACS Appl. Polym. Mater.*, 2024, **6**, 11137–11148.

23 D. Zhao, W. Chen, C. Qu, C. Liu, B. Cui, G. Li, J. Song, L. Li, S. Zheng, J. Chang, Y. Tang, L. Shang and H. Zhang, *J. Appl. Polym. Sci.*, 2019, **136**, 48148.

24 H. Qi, X. Wang, T. Zhu, J. Li, L. Xiong and F. Liu, *ACS Omega*, 2019, **4**, 22143–22151.

25 H.-J. Park, J.-Y. Choi, S.-W. Jin, S.-H. Lee, Y.-J. Choi, D.-B. Kim and C.-M. Chung, *Polymers*, 2022, **14**, 5392.

26 M. B. H. Othman, M. R. Ramli, L. Y. Tyng, Z. Ahmad and H. M. Akil, *Mater. Des.*, 2011, **32**, 3173–3182.

27 J. Q. Li, M. Zeng, X. H. Xu, L. Diao, J. Q. Xie, A. H. Chen, Y. P. Yang and Y. Peng, *High Perform. Polym.*, 2025, **37**, 3–16.

28 J. Han, L. Kiss, H. Mei, A. M. Remete, M. Ponikvar-Svet, D. M. Sedgwick, R. Roman, S. Fustero, H. Moriwaki and V. A. Soloshonok, *Chem. Rev.*, 2021, **121**, 4678–4742.

29 Y.-C. Lin, C.-H. Chiang, C.-C. Kuo, S.-N. Hsu, T. Higashihara, M. Ueda and W.-C. Chen, *J. Appl. Polym. Sci.*, 2019, **136**, 47828.

30 J. Nunoshige, H. Akahoshi, Y. Liao, S. Horiuchi, Y. Shibasaki and M. Ueda, *Polym. J.*, 2007, **39**, 828–833.

31 Y. Seike, Y. Okude, I. Iwakura, I. Chiba, T. Ikeno and T. Yamada, *Macromol. Chem. Phys.*, 2003, **204**, 1876–1881.

32 M. C. Yang, T. Higashihara, H. W. Su, M. Ueda and W.-C. Chen, *J. Polym. Sci., Part A:Polym. Chem.*, 2016, **54**, 3218–3223.

33 A. S. Hay, *J. Polym. Sci.*, 1962, **58**, 581–591.

34 X. Li, T. Liu, Y. Jiao, J. Dong, F. Gan, X. Zhao and Q. Zhang, *Chem. Eng. J.*, 2019, **359**, 641–651.

35 R. Yang, X. Liu, Y. Zhang and Q. Zhuang, *Eur. Polym. J.*, 2024, **203**, 112654.

36 K. Zhang, L. Han, P. Froimowicz and H. Ishida, *Macromolecules*, 2017, **50**, 6552–6560.

37 D.-D. Guo, J.-W. Jiang, Y.-J. Liu, X.-L. Liu and S.-R. Sheng, *J. Fluorine Chem.*, 2015, **175**, 169–175.

38 F. He, K. Jin, J. Wang, Y. Luo, J. Sun and Q. Fang, *Macromol. Chem. Phys.*, 2015, **216**, 2302–2308.

39 C. T. Rosenmaver, J. W. Bartz and J. Hammes, *Mater. Res. Soc. Symp. Proc.*, 1997, **476**, 231–236.

40 N. P. Hacker, G. Davis, L. Figge, T. Krajewski, S. Lefferts, J. Nedbal and R. Spear, *Mater. Res. Soc. Symp. Proc.*, 1997, **476**, 25–30.

41 Q. Wu, W. Zhang, W. Shao, Y. Pei and J. Wang, *Eur. Polym. J.*, 2023, **194**, 112136.

42 J. Wang, J. Zhou, K. Jin, L. Wang, J. Sun and Q. Fang, *Macromolecules*, 2017, **50**, 9394–9402.

43 P. K. Sharma, N. Gupta and P. I. Dankov, *AEU – Int. J. Electron. Commun.*, 2020, **127**, 153455.

44 C. Zhang, D. Wang, J. He, M. Liu, G.-H. Hu and Z.-M. Dang, *Polym. Chem.*, 2014, **5**, 2513–2520.

45 M. Seino, T. Hayakawa, Y. Ishida, M. Kakimoto, K. Watanabe and H. Oikawa, *Macromolecules*, 2006, **39**, 3473–3475.

46 Y. Nakajima and S. Shimada, *RSC Adv.*, 2015, **5**, 20603–20616.

47 D. A. Rooke, Z. A. Menard and E. M. Ferreira, *Tetrahedron*, 2014, **70**, 4232–4244.

48 S. J. Clarson, K. Dodgson and J. A. Semlyen, *Polymer*, 1985, **26**, 930–934.

49 S. Wu, T. Hayakawa, R. Kikuchi, S. J. Grunzinger, M. Kakimoto and H. Oikawa, *Macromolecules*, 2007, **40**, 5698–5705.

50 D. V. Golubenko, E. Y. Safronova, A. B. Ilyin, N. V. Shevlyakova, V. A. Tverskoi, L. Dammak, D. Grande and A. B. Yaroslavtsev, *Mater. Chem. Phys.*, 2017, **197**, 192–199.

51 C. Nam, H. Li, G. Zhang and T. C. M. Chung, *Macromolecules*, 2016, **49**, 5427–5437.

52 Y.-C. Chen, H.-C. Lin and Y.-D. Lee, *J. Polym. Res.*, 2003, **10**, 247–258.

53 H. Liu, R. Sawada, S. Yanagimoto, Y. Yanagimoto and S. Ando, *Appl. Phys. Lett.*, 2024, **124**, 232903.